High-order harmonic generation in cyclic organic molecules

N. Hay,[1,*] M. Castillejo,[2] R. de Nalda,[2] E. Springate,[1] K. J. Mendham,[1] and J. P. Marangos[1]
[1]*The Blackett Laboratory, Imperial College of Science, Technology, and Medicine, London SW7 2BZ, United Kingdom*
[2]*Instituto de Química Física Rocasolano, CSIC, Serrano 119, 28006 Madrid, Spain*
(Received 4 November 1999; published 14 April 2000)

High-order harmonic generation from the interaction of high-intensity femtosecond laser pulses with the organic molecules benzene and cyclohexane has been observed using laser pulses of 240 and 70 fs duration at wavelengths around 800 nm. Harmonic intensities were measured as a function of laser intensity in the range 4×10^{13}–$5\times10^{15}\,\mathrm{W\,cm^{-2}}$, of laser polarization, and of the density of the medium. Harmonics from the 7th to the 13th order were found to have comparable intensities with those produced by xenon at the same density. The 7th harmonic from cyclohexane was measured to be four times more intense than that from xenon. No saturation of this harmonic was observed in cyclohexane up to a peak intensity of $2\times10^{15}\,\mathrm{W\,cm^{-2}}$, in contrast with xenon, where saturation was seen above $8\times10^{14}\,\mathrm{W\,cm^{-2}}$. These results are related to previous studies of ionization and fragmentation of these molecules in the same intensity range. The role of resonances between harmonics and high-lying molecular states is discussed.

PACS number(s): 42.65.Ky

I. INTRODUCTION

Understanding of the interaction of intense laser fields with molecular systems has progressed considerably over the last few years, owing to the attention paid by many groups to complementary aspects of the interaction. Novel phenomena have been observed as a result of this interaction, including molecular ionization and fragmentation [1–20], multiple electron emission, possibly followed by Coulomb explosion [4–7,14,15,18], and extreme ultraviolet (XUV) generation by high harmonic generation (HHG) [21–24]. As compared with atoms, molecules are significantly more complex in their interaction with intense fields due to the presence of additional degrees of freedom involving nuclear motion and the possibility of dissociation. Moreover, molecules introduce the possibility of excitation of additional collective electron effects and of harmonic emission by an electron recolliding with an atom other than its parent. Ionization, fragmentation, and Coulomb explosion have been investigated in diatomic [1–5] and triatomic [6,7] systems and more recently in polyatomic organic molecules [8–20].

Regarding HHG, in comparison with the abundance of work concerning atomic systems, studies in molecules are scarce due to the additional complexity introduced by the molecular structure and to the practical problems of sample handling. For atomic systems the semiclassical two-step description of the process of HHG predicts the maximum harmonic frequency to be determined by the $I_p+3.2U_p$ law [25], where I_p is the ionization potential and U_p the ponderomotive energy. Therefore, although the highest harmonics have been seen in the lightest rare gases with the highest ionization potentials, the most efficient generation of harmonics has been observed in the heaviest elements with their loosely bound outer electrons and consequently greater polarizabilities. This has helped to motivate the investigation of molecules as potential targets for HHG, as many molecular species also have large polarizabilities.

Using a multiphoton-type model, Chin and Golovinski [21] predicted that the intensities of the harmonics for a molecule and an atom with the same ionization potential will be strongly dependent on the ratio between their polarizabilities. Experimental results by Liang *et al.* [22,23] and Lyngå *et al.* [24] have not confirmed this prediction, however. Lyngå *et al.* [24] studied HHG from several polyatomic molecules and found that the conversion efficiency is not higher than that of the rare gases. Organic molecules with delocalised π electrons are thought to be good targets for the study of HHG because of the large nonlinear optical susceptibilities associated with the presence of loosely bound electrons. Indeed, good conversion efficiencies for four-wave mixing processes to generate coherent radiation into the vacuum ultraviolet (VUV) have been reported for a number of double-conjugated systems [26].

In a previous study, we investigated HHG in organic molecules [27] and showed that the systems studied (butane and butadiene) have a conversion efficiency one order of magnitude lower than that of xenon for the same medium density. At intensities of $2.5\times10^{13}\,\mathrm{W\,cm^{-2}}$ harmonics in butadiene were generated with higher efficiency than in butane; this effect was attributed to the presence of π electrons in butadiene.

As a continuation of this work and to further investigate the dependence of HHG processes on molecular properties, such as geometry, size, type of bonding, and the role of electron delocalization, we present here the results of a study performed on the molecules of benzene (C_6H_6) and cyclohexane (C_6H_{12}). Their harmonic response was compared with the rare gas xenon, for which HHG processes are well understood [28–30]. Benzene and cyclohexane have high static polarizabilities of 10.3×10^{-24} and $11.0\times10^{-24}\,\mathrm{cm^3}$, respectively, to be compared with the value of $4.0\times10^{-24}\,\mathrm{cm^3}$ of xenon. Both molecules have similar six-carbon-atom ring structures. Benzene features complete π-electron delocalization, whereas the outer electrons in the cyclohexane

*Corresponding author. Electronic address: n.hay@ic.ac.uk

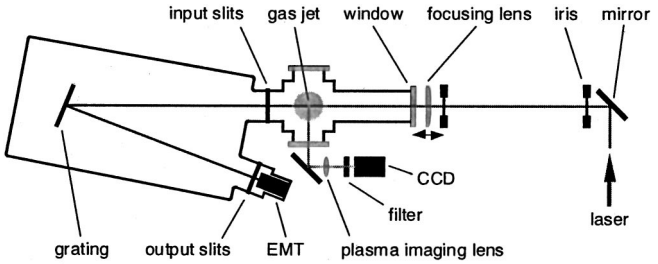

FIG. 1. Experimental layout.

molecule are in σ orbitals. By using laser pulses of 240 fs at 780 nm and 70 fs at 795 nm, the 7th to 15th harmonic orders of the fundamental frequency were generated in the studied media. Their respective signals have been measured as a function of laser intensity, in the range from 4×10^{13} to $5\times10^{15}\,\mathrm{W\,cm^{-2}}$, the laser polarization, and the density of the medium. The results are discussed taking into account the ionization and fragmentation of the molecules over the same intensity range. We consider also the influence of resonances matching the energy of the generated harmonic radiation.

II. EXPERIMENTAL PROCEDURE

The experimental setup, shown in Fig. 1, was based on a system used for previous experiments in the butane and butadiene molecules [27]. For the work reported here, two terawatt Ti:sapphire laser systems employing the technique of chirped pulse amplification were used and will be described below. The first system, at the Blackett Laboratory Laser Consortium, produces a 10 Hz train of 240 fs, 780 nm pulses with energy up to 40 mJ. The second laser was the ASTRA system at the Rutherford Appleton Laboratories, which produces shorter pulses, of about 70 fs, at a center wavelength of 795 nm, a maximum energy of 10 mJ, and a repetition rate of 10 Hz. Both systems produced linearly polarized pulses.

The laser operating at the Blackett Laboratory has been described previously [31] and a short overview is presented here. The Kerr lens mode-locked Ti:sapphire oscillator is pumped by a 5.5 W continuous-wave argon-ion laser (Coherent Innova 100) and delivers an 83 MHz train of 90 fs, 780 nm, 2 nJ pulses, which are stretched to 250 ps in a single-grating singlet-lens pulse stretcher. These pulses are amplified in a Ti:sapphire regenerative amplifier which selects a 10 Hz pulse train from the 83 MHz stretched oscillator output. The energy of the pulses is amplified by a factor of 10^6 to 2 mJ. The crystal is pumped at 10 Hz by 90 mJ pulses from a frequency-doubled *Q*-switched Nd:YAG (yttrium aluminum garnet) laser (Continuum Surelite II). Further amplification of the stretched pulses is achieved in a five-pass, angularly multiplexed amplifier pumped by 400 mJ pulses from a frequency-doubled *Q*-switched Nd:YAG laser (BMI 503). This increases the energy up to 80 mJ before recompression in a grating pulse compressor. An energy loss of $\sim$50% is incurred by passing through the compressor, making the maximum final energy of the pulses 40 mJ.

The ASTRA system had a similar configuration to the laser described above, although the regenerative amplifier was replaced by a multipass amplifier. To support shorter pulses the bandwidth of the ASTRA system was 23 nm, almost three times greater than the $\sim$8 nm bandwidth of the Blackett Laboratory system.

The pulse duration at the output of the laser systems was measured to be 240 and 70 fs for the Blackett Laboratory and ASTRA systems, respectively, using a second-order autocorrelator and assuming a sech^2 pulse shape. The pulse energy was obtained from a calibrated photodiode.

The laser output was focused into a gas jet of the species under study using a 300 mm focal length antireflection- (AR-) coated fused silica planoconvex lens. Because of the different beam diameters of the two lasers used in this work, the focusing geometry changed from $f/11$ for the Blackett Laboratory system to $f/19$ for the ASTRA system. The peak intensity in the focus was determined by combining measurements of the pulse energy and duration with a measurement of the e^{-2} area of the spatial intensity distribution of an attenuated beam in the focal plane of the focusing lens. A 1 mJ pulse was found to produce a peak intensity in the focus of $1\times10^{14}\,\mathrm{W\,cm^{-2}}$ for the Blackett Laboratory system and $4\times10^{13}\,\mathrm{W\,cm^{-2}}$ for ASTRA. The relative error in peak intensity between experiments was less than 25%. This was achieved by carefully maintaining a fixed experimental arrangement and was proven by the extremely good agreement between the results of identical experiments carried out on different days. However, the error in the absolute peak intensity was quite large (we estimate a factor of 5). This was primarily due to the assumption of a Gaussian transverse intensity distribution, whereas the actual distribution in the focus has higher intensity in the wings than an ideal Gaussian.

The intensity in the laser focus was varied by adjusting the pulse energy. This was achieved by using an electronically controlled $\lambda/2$ waveplate combined with a fused silica cube polarizer, which attenuated the pulses at the output of the regenerative amplifier. In this way the intensity in the focus could be varied over more than two orders of magnitude. Where a constant intensity was required for an experiment the digitized, integrated signal from the diode monitoring the pulse energy at the experiment was passed to the data acquisition computer. This then accepted the corresponding harmonic signal as a valid datum or rejected it depending on whether the energy (intensity) was within a predefined range (typically $\pm5\%$ of the mean value). This process, termed ''energy binning,'' was essential because of the often highly nonlinear scaling of harmonic signal with laser energy. Where the harmonic signal was examined as a function of intensity, the same technique was used except that many adjacent energy bins (ranges) were defined and the harmonic signal was allocated to the appropriate bin rather than discarded. Typically, the bins were evenly spaced on a logarithmic scale to optimize the signal-to-noise ratio over a large range of laser intensities.

The gas jet was produced by a heated pulsed valve mounted on top of a small vacuum chamber with four 4-cm-diameter ports in the horizontal plane arranged on two perpendicular axes. One port was directly connected to a VUV monochromator. The laser pulses were focused through the opposite port, which was fitted with an extension tube to

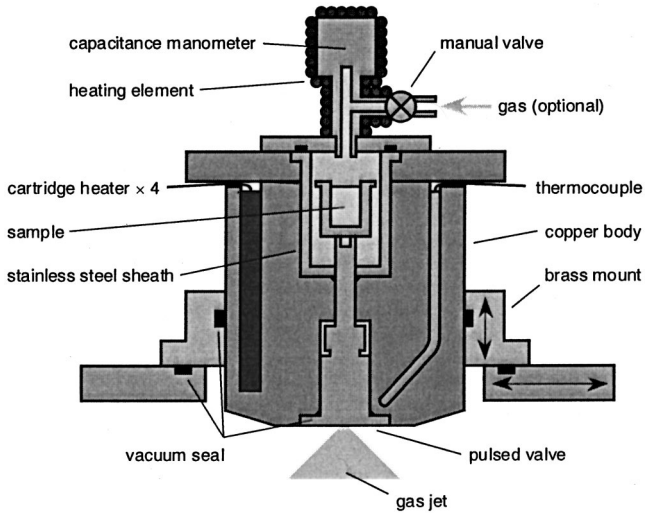

FIG. 2. Temperature-controlled pulsed gas valve with integrated sample reservoir and pressure monitoring.

locate the 3-mm-thick fused silica AR-coated entrance window as near as possible to the focusing lens. The two remaining ports were fitted with fused silica windows to allow inspection of the interaction region perpendicular to the direction of laser propagation. One of these ports was used to image the plasma emission from the interaction region onto a charge-coupled device (CCD) camera (Pulnix TM500).

A heated pulsed gas valve system, depicted in Fig. 2, was built and used to generate gas jets of benzene and cyclohexane, which are liquids at room temperature. It consisted of an integrated solenoid pulsed valve (General Valve Corp., Series 9) and a sample reservoir that were temperature controlled up to 470 K with a temperature stability of ± 0.1 K. The vapor pressure created in the reservoir was measured by a heated capacitance manometer; its temperature was monitored by a type-*K* thermocouple and maintained slightly higher than the temperature of the rest of the heated valve to ensure that no condensation occurred. This allowed us to directly determine, in a manner independent of the species, the backing pressure on the pulsed valve.

To compare the efficiencies of the harmonics in the organic compounds with those generated in xenon, we ensured that the target gas density in the interaction region was the same for all the species studied. A gas backing pressure of 220 Torr of xenon implied a density of 3×10^{17} atoms cm^{-3} in the laser focus, which was 3.2 mm below the nozzle throat, providing an interaction length of $\sim$6 mm. The ratio γ of the specific heat capacity at constant pressure to that at constant volume for benzene and cyclohexane is around 1.6 times lower than that of xenon. Therefore, to produce the same density of molecules in the interaction region, the backing pressure used for both compounds had to be three times greater than for xenon, i.e., 660 Torr. A sonic expansion into perfect vacuum with an expansion half angle of 45° was assumed for the calculation. To obtain the required backing pressure of the organic compounds, the heated pulse valve ensemble had to be maintained at 350 K.

The density in the gas jet was chosen to avoid defocusing of the fundamental beam in the jet and to minimize the risk of an accidental release of organic vapor to the atmosphere by keeping the required valve backing pressure below atmospheric pressure. We set the position of the laser focus in the gas jet by optimizing the 9th harmonic yield in xenon.

Benzene and cyclohexane samples (Aldrich Ltd.) had a purity better than 99.9% and were used without further purification. Xe (BOC Ltd.) had a specified purity of 99.993%.

The harmonics generated in the laser focus were resolved by a 1 m normal-incidence VUV monochromator (GCA McPherson 225) fitted with an aluminum-coated 600 lines mm^{-1} grating. The harmonics were detected using an electron multiplier tube (EMT, Thorn EMI 143) operated at 2.5 kV and positioned behind the exit slit in the image plane of the monochromator. A stepper motor was fitted to the wavelength selection dial to rotate the grating and select the wavelength. A boxcar-gated integrator (Stanford Research SR 250) integrated the signal output from the electron multiplier and from a laser pulse energy monitor diode after every laser pulse. These measurements were digitized and transferred to a PC via an RS-232 serial link. Data acquisition software running on the PC was configured to perform signal averaging and laser energy binning as required. The data acquisition software also controlled the monochromator wavelength via a stepper-motor interface.

III. RESULTS

Two series of experiments were carried out using 240 and 70 fs laser pulses delivered by the laser systems described in the previous section. The first series were obtained in the 1.5×10^{14}–5×10^{15} W cm^{-2} intensity range with 240 fs, 780 nm laser pulses. The second series covered the 4×10^{13}–5×10^{14} W cm^{-2} intensity range with 70 fs, 795 nm laser pulses.

A. VUV spectra of harmonic generation

Harmonic spectra were recorded for benzene, cyclohexane, and xenon. The results obtained with 240 fs pulses at 2×10^{15} W cm^{-2} are shown in Fig. 3. Each spectrum consists of 1100 points, each recorded point being the average of the signal generated by 20 laser pulses. Only pulses having an energy within $\pm 7\%$ of the target energy were permitted to contribute to the mean value. Ten-point adjacent average smoothing was applied to all spectra in Fig. 3 to reduce the noise level. The width of the peaks in the recorded spectra was limited by the instrumental resolution to 2 nm. The spectra have not been corrected for the spectral response of the detection system. This prevented us from comparing the absolute signal strengths of different peaks in the spectra. However, a reference xenon spectrum was recorded immediately prior to each of the molecular spectra to ensure that absolute comparisons between the responses of each medium for a given harmonic order were possible.

Harmonic orders $q=7$ to 13 are present in the spectra. The most striking feature of these data is that the strengths of the harmonic signals from the organic molecules are comparable to those from xenon atoms. Xenon is one of the most efficient HHG media studied to date in this intensity range; it

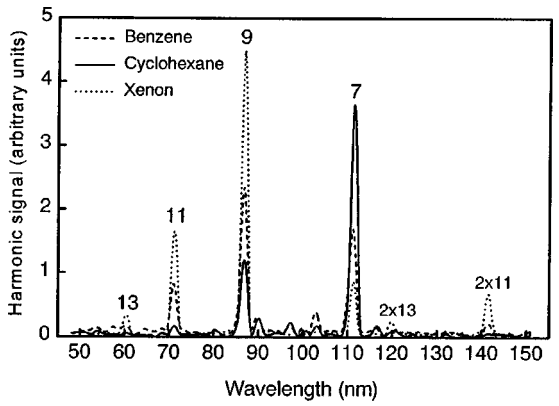

FIG. 3. Harmonic spectra for benzene (— — —), cyclohexane (—), and xenon (···) produced by 240 fs, 780 nm laser pulses focused to a peak intensity of $2\times10^{15}\,\mathrm{W\,cm^{-2}}$. The density in the interaction region was $\sim3\times10^{17}\,\mathrm{molecules\,cm^{-3}}$. Harmonics of the 7th to the 13th order are detected. Small peaks from second-order diffraction of the 11th and 13th harmonics can also be seen.

is remarkable, therefore, that the 9th and 11th harmonics of the organic compounds are up to 50% as strong as those of xenon and that the 7th harmonic of cyclohexane is up to four times stronger. In this case, no harmonics above $q=11$ were measured from either benzene or cyclohexane.

Peaks are also present in the spectra from second-order diffraction of the 11th and 13th harmonics. Several further small peaks appear in the benzene and cyclohexane spectra, mainly at wavelengths between the 7th and 9th orders of the laser frequency; these peaks are absent in the xenon spectra. Similar features were also observed in the HHG spectra of butane and butadiene [27]. The temporal profile of these emissions was measured and presented a slow decay with an effective lifetime of the order of several tens of nanoseconds, in contrast with the prompt emission of harmonic photons. We attribute these emissions to recombination of the ions and electrons in the plasma formed as the laser pulse propagates through the nonlinear medium. The observed features could be identified as emission lines from neutral hydrogen and neutral and singly ionized carbon atoms. This would explain the absence of these peaks in the xenon spectra.

Harmonics spectra were also recorded using 70 fs, 795 nm pulses from the ASTRA system. The increased dynamic range of this system allowed the detection of the 13th harmonic from both organic molecules and of the 15th harmonic in xenon. Consistent with the 240 fs pulses results, the harmonic spectra of benzene and cyclohexane follow the same trend, having a higher 7th harmonic yield than xenon and somewhat lower yields at higher orders. Cyclohexane was generally less efficient than benzene, but again it had an exceptionally high yield at $q=7$, four times higher than the xenon yield. The peaks attributed to plasma emission are weaker than those observed with 240 fs, as the lower intensity and shorter pulse duration reduce ionization.

B. Harmonic-generation dependence on laser intensity

We investigated the dependence of HHG in benzene, cyclohexane, and xenon upon the intensity of the driving laser. This was done by setting the monochromator at the desired harmonic wavelength and varying the laser energy. Each intensity dependence consisted of data from around 6000 laser pulses.

Figure 4 shows the intensity dependences for harmonics $q=7-13$ in xenon and $q=7-11$ in benzene and cyclohexane using 240 fs pulses. A log-log curve of the harmonic signal versus laser intensity is plotted for each harmonic. The 13th harmonic was too weak to be detected in the organic molecules. Because the harmonic detection system was not calibrated absolutely, the relative yield of the harmonic orders is unknown and so their relative position on the vertical axis is arbitrary. The curve of harmonic signal versus intensity for each order was scaled by a constant factor, so they overlapped at low intensity where their behavior was identical. This clarifies the divergent behavior that occurs at higher intensity without resulting in a loss of information about the relative harmonic yields, because this information is contained in the VUV spectra shown in Fig. 3. The observed dependences were fitted by power laws as shown in Fig. 4.

Xenon harmonics yields presented in Fig. 4(c) show the characteristic behavior with intensity usually observed in HHG [28–30]. There is an initial steep dependence on intensity followed by saturation at intensities over $8\times10^{14}\,\mathrm{W\,cm^{-2}}$. The intensity dependences of the xenon harmonics were identical across the observed intensity range.

The intensity dependences of benzene harmonics are shown in Fig. 4(a). As with xenon, all the harmonic signals first increase with a slope around 2 on a log-log scale, before beginning to roll over as the intensity approaches $7\times10^{14}\,\mathrm{W\,cm^{-2}}$. At this point the intensity dependences of the different harmonics diverge. The rollover is most pronounced for $q=7$ and is reduced for higher q. Above $2\times10^{15}\,\mathrm{W\,cm^{-2}}$ and up to $4\times10^{15}\,\mathrm{W\,cm^{-2}}$ this tendency is reversed, with the lower-order harmonics showing the steepest intensity dependence.

For cyclohexane [Fig. 4(b)] all harmonics again follow the same initial intensity dependences, whereas above $1\times10^{15}\,\mathrm{W\,cm^{-2}}$ the curves diverge. The 11th harmonic rolls over to become almost constant with increasing intensity. There is no change of slope in the 9th harmonic, and the 7th harmonic actually exhibits a steeper intensity dependence without signs of saturation. This is in marked contrast with xenon [Fig. 4(c)], where all the harmonic orders have saturated at this intensity.

Figure 5 depicts the intensity dependences of the harmonic signals generated with 70 fs pulses also scaled by a constant factor as described previously. Although the intensity range covered in this experiment is smaller, the better detection dynamic range enabled us to measure the weaker 13th harmonic of the organic molecules and also to observe an initial steep intensity dependence of the harmonic signal. Where the intensity ranges of the two experiments overlap, we can see that the behavior of all the molecules appears to be similar. The intensity dependences follow a quadratic power law in the $(2-4)\times10^{14}\,\mathrm{W\,cm^{-2}}$ intensity range (with the exception of $q=11$ for cyclohexane using 70 fs pulses). Therefore in this range shortening the pulse duration did not affect the observed dependences appreciably.

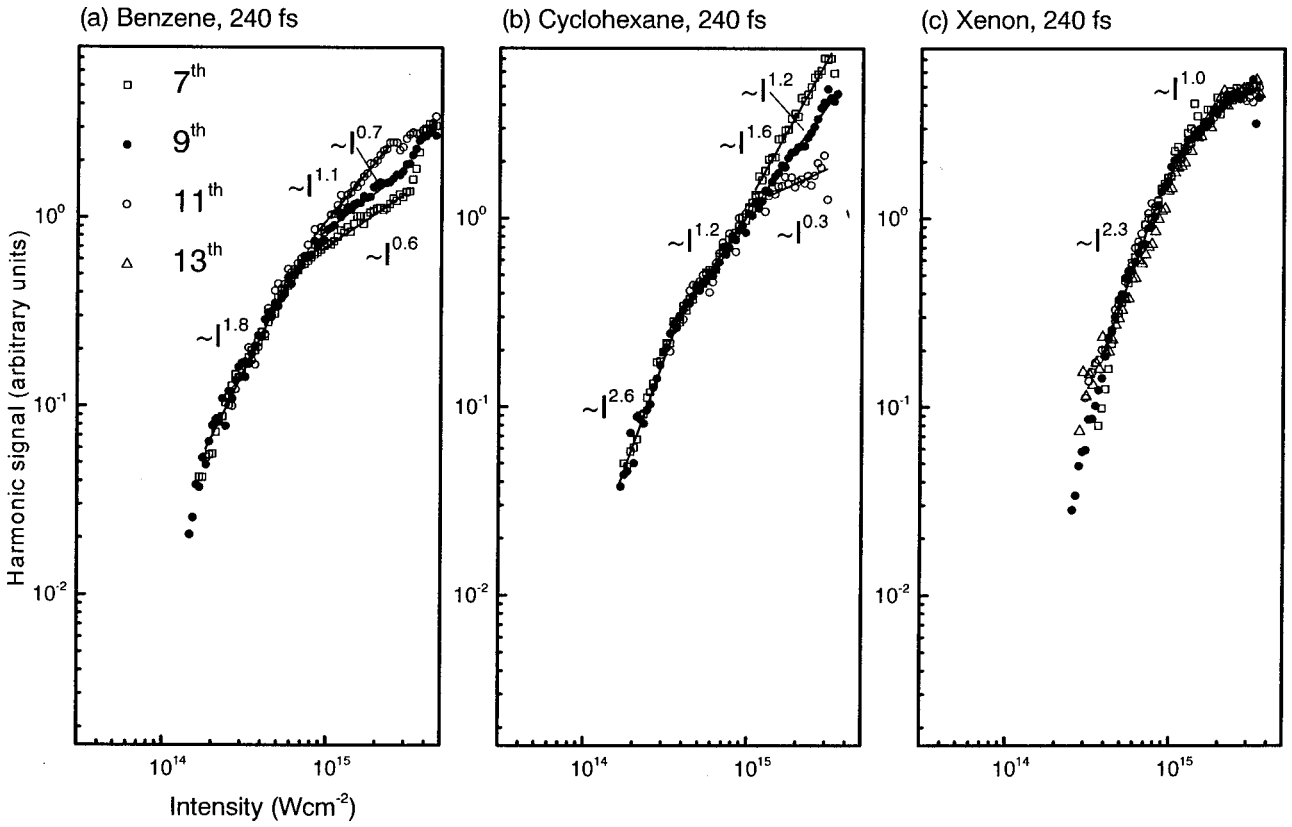

FIG. 4. Harmonic intensity for (a) benzene, (b) cyclohexane, and (c) xenon as a function of laser intensity for $q=7-13$ using 240 fs, 780 nm laser pulses in the intensity range $1.5\times10^{14}-5\times10^{15}\,\mathrm{W\,cm^{-2}}$. The density in the interaction region was $\sim3\times10^{17}\,\mathrm{molecules\,cm^{-3}}$. Each harmonic has been scaled vertically as described in the text.

C. High-order harmonic dependence on ellipticity of laser polarization

We also compared the dependence of harmonic yield on the ellipticity of the laser beam for the organic molecules and xenon. Figure 6 shows the results for the 7th and 11th harmonics of xenon and benzene at a peak intensity of $3\times10^{15}\,\mathrm{W\,cm^{-2}}$. For both species, the ellipticity dependence is stronger for the higher-order harmonic. The results also show that the harmonic yield in benzene decreases more rapidly with ellipticity than for xenon atoms. The generation of high harmonics is very sensitive to the polarization of the pump laser [32]. This is intuitively obvious in the recollision model of HHG; for linear polarization, the electron wave packet is driven in a one-dimensional trajectory away from the parent atom before returning with a high probability of recollision. If the laser is elliptically polarized then there will be an additional transverse component to the force on the electron wave packet, and the probability of recollision is reduced. According to this model, a greater ellipticity leads to a smaller recollision probability and to a lower harmonic yield. The results shown here could imply that the collision cross section of xenon is larger than that of benzene. This is reasonable if in benzene HHG arises only from the electron wave packet recolliding with its parent atom and not with the molecule as a whole.

D. Harmonic-generation dependence on medium density

The harmonic yield was studied as a function of the density of the nonlinear medium. The density in the gas jet was controlled by varying the backing pressure. Sets of data for the 7th harmonic at the intensity of $3\times10^{15}\,\mathrm{W\,cm^{-2}}$ from the species studied in this work were obtained by averaging the signal from 200 laser pulses with a 5% energy bin as a function of the backing pressure. In a log-log representation the data could be fitted by single straight lines with a slope near 2. The observed dependences are in good agreement with the quadratic law expected for a phase-matched HHG process [28].

IV. DISCUSSION

The highest harmonic order detected in xenon was $q=13$ with the 240 fs laser at $5\times10^{15}\,\mathrm{W\,cm^{-2}}$ and $q=15$ with the 70 fs laser at $5\times10^{14}\,\mathrm{W\,cm^{-2}}$. These limits were imposed by the short-wavelength response of the detection system. Therefore it was not possible to determine experimentally the position of the cutoff for xenon. This cutoff can be calculated through the $I_p+3.2U_p$ rule. However, there is a maximum laser intensity to which a neutral atom may be exposed before it ionizes. This maximum intensity is set by the barrier suppression ionization (BSI) limit [33] and for xenon is $9\times10^{13}\,\mathrm{W\,cm^{-2}}$. A xenon atom exposed to this intensity will ionize within a single optical cycle. Harmonics up to $q=17$ could be generated in xenon at this intensity. Below this value ionization can proceed through multiphoton and tunneling ionization. Considering tunneling ionization, modeled by the Ammosov, Delone, and Krainov (ADK)

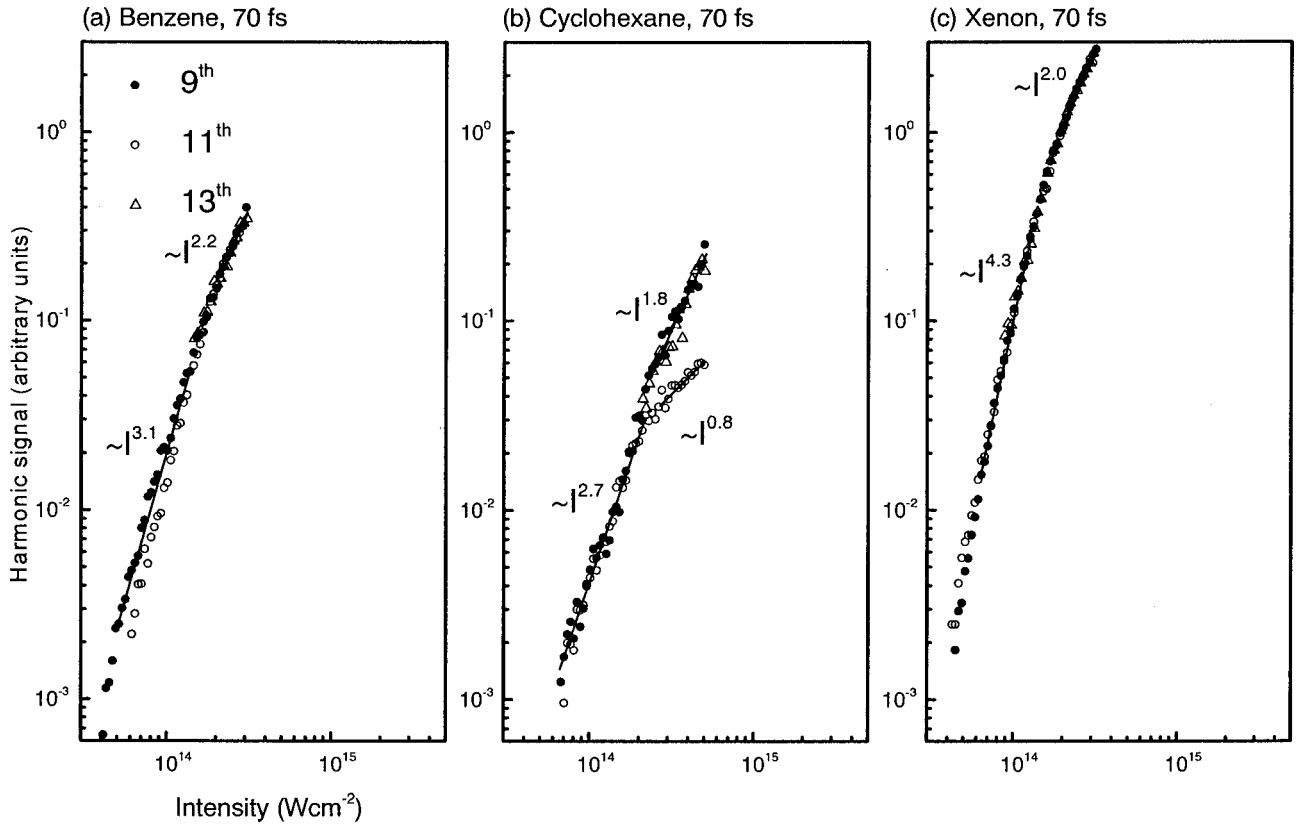

FIG. 5. As in Fig. 4 for $q=9-13$ using 70 fs, 795 nm laser pulses in the intensity range $4\times10^{13}-5\times10^{14}\,\mathrm{W\,cm^{-2}}$. The density in the interaction region was $\sim3\times10^{17}$ molecules $\mathrm{cm^{-3}}$.

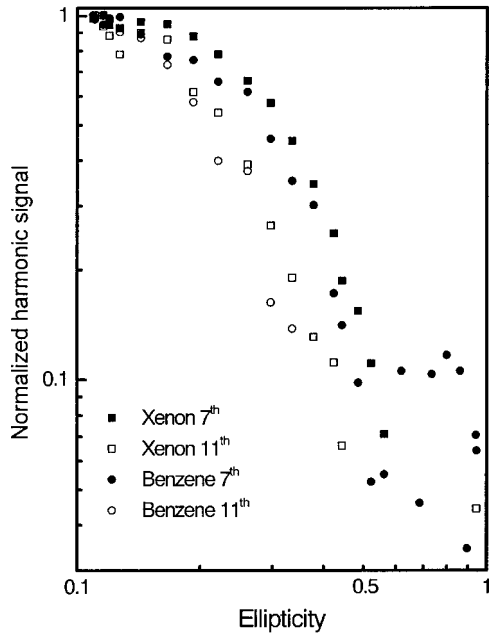

FIG. 6. Dependence of benzene (circles) and xenon (squares) 7th (solid symbols) and 11th (open symbols) harmonic yields as a function of the ellipticity of the pump beam for 240 fs, 780 nm pulses at a laser intensity of $3\times10^{15}\,\mathrm{W\,cm^{-2}}$. Each set of data has been normalized to unity.

rates [34], the saturation intensity for Xe^+ is $\sim6\times10^{13}\,\mathrm{W\,cm^{-2}}$ for 70 fs pulses and slightly less for 240 fs pulses. The corresponding cutoff occurs at $q=13$. The fact that harmonics are observed at peak intensities up to $3\times10^{15}\,\mathrm{W\,cm^{-2}}$ is due to emission during the rising edge of the laser pulse before ionization has saturated and also from the wings of the focus where ionization does not reach saturation [35].

For both laser pulse durations, the highest-order harmonics observed in benzene and cyclohexane were one order lower than those observed from xenon. The cutoff occurred in both cases also at lower orders than predicted by the $I_p+3.2U_p$ rule, suggesting that the molecules were being ionized before the peak of the pulse was reached.

Comparison of the laser intensity dependences of harmonics yields in xenon, benzene, and cyclohexane reveals the role of the macroscopic phase mismatch and the microscopic susceptibility [28,36]. The phase mismatch arises from three terms: the focal geometry, the difference in the dispersion of the neutral gas at the fundamental frequency and the harmonic frequency, and finally the effect of free electrons. During the experiments the same focal geometry was used throughout; therefore this term is constant for all the studied media. The dispersion term is small as compared with the other two and can be neglected [23] provided that the harmonic frequency is far from the vicinity of resonances. This

condition is fulfilled in these experiments for the case of xenon but not for the benzene and cyclohexane systems, which present numerous resonances in the VUV region covered by the generated harmonics. Moreover, the molecular excited states could be shifted into harmonic resonances by the ac Stark effect. This point will be elaborated below. The laser intensity determines to what extent the medium is ionized; therefore at high laser intensity, when the gas is strongly ionized, the effect of free-electron dispersion will be important and even dominate the phase mismatch. Because the gases studied in this experiment have different ionization potentials (9.24, 9.86, and 12.13 eV for benzene, cyclohexane, and xenon, respectively) the free-electron density created from the ionization of each species should be different.

The microscopic susceptibility characterizes the response of each individual atom or molecule to the radiation field. Resonances of the generated harmonics with excited states of the neutral atom or molecule will strongly modify the value of the susceptibility. However, although at low laser intensity neutral atoms or molecules will be responsible for generating high harmonics, increasing the intensity will result in single ionization or multiple ionization of the species, and dissociation in the case of molecules. Therefore the effects of both neutral depletion and contribution of ions or fragments to the overall process of HHG have to be taken into account.

The harmonic intensity dependences shown in Figs. 4 and 5 for xenon consist of three stages, each with a characteristic slope [30]. In the first stage, at the lowest intensities below $1\times10^{14}\,\mathrm{W\,cm^{-2}}$, the slope is steepest and the dependence can be fitted by an $\sim I^4$ law. This regime, which corresponds to harmonics in the cutoff region, could be observed only in the experiments using 70 fs pulses, because the harmonic signal was too weak to be distinguished from the noise in the 240 fs experiments. As the harmonic moves to the plateau region, a second stage is accessed in which the intensity dependence is reduced. In the range $(2-8)\times10^{14}\,\mathrm{W\,cm^{-2}}$ all the harmonics from xenon appear to be in the plateau characterized by a quadratic intensity dependence. Above $8\times10^{14}\,\mathrm{W\,cm^{-2}}$ the harmonic intensity dependence steadily flattens out until the harmonic signal is almost constant with intensity at $3\times10^{15}\,\mathrm{W\,cm^{-2}}$. This was accompanied by the observation of plasma emission from the laser focus by the CCD camera that monitors the interaction region, and is indicative of significant ionization of the medium. Only the experiments with the 240 fs laser achieved sufficient intensity to observe this regime. This third stage is brought about by ionization of the nonlinear medium, which further decreases the slope as the neutral harmonic emitters are depleted and the free electrons have a detrimental effect on the phase matching.

The main effect of ionization is to deplete the number of neutral atoms available for harmonic generation. As the density of atoms is low in the interaction region and the laser is tightly focused in our case, the phase mismatch due to dispersion in the focus is dominated by the geometric phase term and not by the dispersion of the free electrons. This is supported by the observed intensity dependences. While the free-electron dispersion is frequency dependent, the behavior as a function of the intensity remains identical across all the harmonic orders studied in the ionization regime.

Like xenon, benzene exhibits a steep intensity dependence below $10^{14}\,\mathrm{W\,cm^{-2}}$ when the harmonics are in the cutoff regime. The low signal levels restricted observation of this regime to the 70 fs experiments, except perhaps for the 9th harmonic, where some of the signal detected around $(1.5-2)\times10^{14}\,\mathrm{W\,cm^{-2}}$ appears to have the characteristic steep intensity dependence. Again like xenon, above $2\times10^{14}\,\mathrm{W\,cm^{-2}}$, the intensity dependence flattens out following a quadratic law, indicating that the harmonics begin to reach the plateau. The transition to saturation occurs in xenon at $\sim8\times10^{14}\,\mathrm{W\,cm^{-2}}$; in benzene the change of slope occurs at slightly lower intensity, $6\times10^{14}\,\mathrm{W\,cm^{-2}}$, above which the intensity dependences differ considerably from those of xenon.

Above $6\times10^{14}\,\mathrm{W\,cm^{-2}}$ each harmonic has a different intensity dependence, the curves becoming steeper as the harmonic order increases. This is opposite to the expected consequence of free-electron dispersion, which would be larger at shorter wavelengths i.e., higher harmonic order. Around $3\times10^{15}\,\mathrm{W\,cm^{-2}}$ the situation reverses, so that the 7th harmonic now has the steepest slope and the 11th becomes almost constant with intensity. This is in contrast with the behavior shown by xenon harmonics, which have completely saturated at this intensity.

The effect of resonances between harmonic frequencies and molecular states has to be considered. The frequencies of the 7th to 11th harmonics are in energy regions corresponding to two Rydberg series of the benzene molecule converging to the 11.48 and 16.48 eV limits [37]. The 9th harmonic is $\sim2300\ \mathrm{cm^{-1}}$ below the start of the series converging to the 16.48 eV limit. When the harmonics are in the region of discrete excited states, the variation of the refractive index will become very large in the vicinity of resonances. This may lead to a breakdown of the phase-matching condition and also to reabsorption of the generated light. Additionally, for the high radiation fields present in this work, the ac Stark effect must be taken into account, as it is strong enough to shift the energy of molecular transitions to be in resonance with the harmonic frequencies. After the resonance is passed at higher intensity, the phase mismatch by dispersion would vanish. These effects result in the appearance of structures on the intensity dependence curve in the vicinity of resonances. This phenomenon [36,38] has been suggested to contribute to the behavior observed in some diatomic systems [23] and could explain the slope change on the intensity dependence curve of the harmonic signal observed in benzene in the range of $(1-5)\times10^{15}\,\mathrm{W\,cm^{-2}}$. The absence of structure in the intensity dependences of the harmonics from xenon is due to the low density of atomic states in the energy region covered by the generated harmonics.

Ion spectroscopic studies of benzene and cyclohexane irradiated by ultrashort high-intensity pulses can help to determine the state of the molecules during the harmonic-generation process. For the laser wavelengths, pulse duration, and intensities characteristic of this work, ionization of the neutral benzene and cyclohexane molecules has been reported by several authors [8–14,16,17]. Formation of

multiply charged parent ions has also been reported to occur at intensities above $10^{14}\,\mathrm{W\,cm^{-2}}$ [14,17]. As the ionization potential of benzene is lower than that of xenon, we would expect ionization to occur at lower intensities in the molecule than in xenon. This is reflected in the intensity dependences by the lower intensity at which the benzene harmonic signals deviate from the plateau behavior. Ionization can be detrimental to HHG both through the depletion of the neutral species and by disruption of the phase-matching condition by free-electron dispersion. Depletion of the neutral species by production of ions is generally undesirable. Harmonic generation from ions is often assumed to be negligible in comparison with that from neutral species because the polarizability of the ion is reduced due to more tightly bound outer electrons. However, other authors [30,39] have suggested that molecular ions might be a more efficient source of harmonic conversion than neutrals because of the larger ionization potential. In the case of benzene, the formation of ions might have a positive influence on the harmonic yield; first, because the loss of one electron from the cloud of π-delocalized electrons will have a much smaller effect on the polarizability of the molecule and second, because the ion ionization potential is larger than in the neutral molecule. In experiments where the free-electron dispersion does not dominate phase matching, this could explain the absence of saturation of high harmonic generation in benzene.

In addition to ionization, benzene may undergo dissociation. The threshold intensity for dissociation has been found to be around $10^{14}\,\mathrm{W\,cm^{-2}}$ [14,17]. As dissociation of benzene certainly takes place in the interaction, we must assume that harmonics are generated also in molecular fragments [24] formed following dissociation of the excited parent ion.

Cyclohexane also appears to exhibit the three characteristic stages of intensity dependence. The transition to a less steep intensity dependence characteristic of the plateau seems to occur at $\sim 2\times10^{14}\,\mathrm{W\,cm^{-2}}$ and from plateau to ionization at $\sim 4\times10^{14}\,\mathrm{W\,cm^{-2}}$, though the overlap between the 70 and 240 fs results is not as good as for benzene and xenon. As with benzene, the harmonic-generation process does not saturate in cyclohexane as the intensity is increased, and again this may be attributed to harmonic generation from ions. The dissociation threshold intensity for cyclohexane has been found to be approximately a factor of 5 lower than for benzene [16,17]. The resulting ion spectrum in cyclohexane is dominated by smaller fragments, in contrast with the benzene spectrum where the parent molecular ion is always the most abundant species. Just above $1\times10^{15}\,\mathrm{W\,cm^{-2}}$ each harmonic behaves differently, with a steeper dependence as the harmonic order decreases. This is opposite to the trend observed in benzene at $6\times10^{14}\,\mathrm{W\,cm^{-2}}$, where the slope increases with increasing harmonic order, but coincides with the behavior in benzene above $3\times10^{15}\,\mathrm{W\,cm^{-2}}$.

Again, the effect of molecular resonances upon the harmonic behavior with laser intensity has to be taken into account. For the case of cyclohexane, two broad features are present in the absorption spectrum of the molecule. A broad-linewidth structure carrying a very high oscillator strength at 10.4 eV has been discussed as one of the rare examples of a molecular giant resonance; the second broad feature occurs at 15.5 eV [40]. Harmonics of 7th and 9th orders are in resonance with the broad absorption bands centered at 10.4 and 15.5 eV, respectively. The stronger dependence on intensity of the 7th harmonic in cyclohexane compared to that in xenon could be related to the presence of the giant resonance. This could also explain the exceptionally high yield of the 7th harmonic which, as described in the previous section, was measured to be four times higher than in xenon.

One possible explanation for the intensity dependences above $3\times10^{15}\,\mathrm{W\,cm^{-2}}$ in benzene and $1\times10^{15}\,\mathrm{W\,cm^{-2}}$ in cyclohexane is that further ionization is occurring and the free-electron dispersion, proportional to the electron density, is beginning to dominate the phase matching. For a fully doubly ionized plasma, the free-electron contribution to the phase mismatch is comparable to the geometrical contribution. This situation could arise through double ionization of the parent molecular ions or by multiplication of the number of ions due to dissociation. The dispersive free electrons introduce a positive phase mismatch between the harmonic and fundamental fields that increases with frequency, which would explain the lower slopes observed for higher-order harmonics.

V. SUMMARY AND CONCLUSIONS

We have studied HHG in the organic molecules benzene and cyclohexane using near-infrared 70 and 240 fs duration laser pulses in the intensity range from 4×10^{13} to $5\times10^{15}\,\mathrm{W\,cm^{-2}}$. Harmonics from the 7th to the 15th order were detected using a normal-incidence VUV monochromator. The harmonic signals were studied as a function of laser intensity, laser polarization, and density of the nonlinear medium. The results were compared with harmonics produced by xenon under nominally identical conditions. The primary result is that the efficiency of harmonic generation for these orders in the organic molecules is comparable with harmonic generation in xenon. No attempt was made to optimize the harmonic conversion efficiency of the organic molecules. We expect that the conversion efficiencies of all of the media would be increased by increasing the density in the laser focus beyond that used here. Under the conditions of this work, cyclohexane seems to present some degree of selectivity for harmonic generation: the 7th harmonic from this molecule was measured to be four times more intense than that of xenon. This high yield could be possibly related to the higher polarizability of the molecule, almost three times that of xenon, and to the presence of a giant resonance in its VUV absorption spectrum.

At high intensity, above $5\times10^{14}\,\mathrm{W\,cm^{-2}}$, the organic molecules behave very differently from the monatomic gas. The usual saturation of the harmonic signal, which is observed as the intensity is increased and the medium becomes fully ionized, is strongly modified in both organic molecules. The structures observed in the intensity dependence curves appear to result from the combination of various effects on the phase mismatch and from the characteristics of the single-particle response. On one hand, molecular states brought into resonance with the harmonic frequency by the ac Stark effect induce changes in the phase mismatch. On the

other hand, single and multiple ionization of the medium and the formation of ionic fragments induce a non-negligible free-electron dispersion term to the phase mismatch and at the same time modify the characteristics of the nonlinear medium. More work is in progress with the molecules studied in this work and in other hydrocarbons using shorter laser pulses of 50 fs duration and higher intensity to elucidate the contribution of the above-mentioned effects to the HHG processes.

ACKNOWLEDGMENTS

We gratefully acknowledge the contributions of J. W. G. Tisch, M. B. Mason, J. P. Connerade, M. H. R. Hutchinson, P. F. Taday, E. Duvall, and A. J. Langley and the technical assistance of P. Ruthven and A. Gregory. This work was supported by the EPSRC and by a British-Spanish Acción Integrada. R. de Nalda acknowledges the Ministerio de Educacion y Cultura (Spain) for financial assistance.

[1] P. Dietrich and P. B. Corkum, J. Chem. Phys. **97**, 3187 (1992).
[2] T. D. G. Walsh, F. A. Ilkov and S. L. Chin, J. Phys. B **30**, 2167 (1997).
[3] M. R. Thompson, M. K. Thomas, P. F. Taday, J. H. Posthumus, A. J. Langley, L. J. Frasinski, and K. Codling, J. Phys. B **30**, 5755 (1997).
[4] C. Guo, M. Li, J. P. Nibarger, and G. N. Gibson, Phys. Rev. A **58**, R4271 (1998).
[5] J. H. Posthumus, J. Plumridge, P. F. Taday, J. H. Sanderson, A. J. Langley, K. Codling, and W. A. Bryan, J. Phys. B **32**, L93 (1999).
[6] Ph. Hering and C. Cornaggia, Phys. Rev. A **59**, 2836 (1999).
[7] J. H. Sanderson, A. El-Zein, W. A. Bryan, W. R. Newell, A. J. Langley, and P. F. Taday, Phys. Rev. A **59**, R2567 (1999).
[8] M. J. DeWitt and R. J. Levis, J. Chem. Phys. **102**, 8670 (1995).
[9] M. J. DeWitt, D. W. Peters, and R. J. Levis, Chem. Phys. **218**, 211 (1997).
[10] M. J. DeWitt and R. J. Levis, J. Chem. Phys. **108**, 7045 (1998).
[11] M. J. DeWitt and R. J. Levis, Phys. Rev. Lett. **81**, 5101 (1998).
[12] R. J. Levis and M. J. DeWitt, J. Phys. Chem. A **103**, 6493 (1999).
[13] K. W. D. Ledingham, D. J. Smith, R. P. Singhal, T. McCanny, P. Graham, H. S. Kilic, W. X. Peng, S. L. Wang, A. J. Langley, P. F. Taday, and C. Kosmidis, J. Phys. Chem. A **102**, 3002 (1998).
[14] K. W. D. Ledingham, R. P. Singhal, D. J. Smith, T. McCanny, P. Graham, H. S. Kilic, W. X. Peng, A. J. Langley, P. F. Taday, and C. Kosmidis, J. Phys. Chem. A **103**, 2952 (1999).
[15] C. Cornaggia, Phys. Rev. A **52**, R4328 (1995).
[16] M. Castillejo, S. Couris, E. Koudoumas, and M. Martin, Chem. Phys. Lett. **289**, 303 (1998).
[17] M. Castillejo, S. Couris, E. Koudoumas, and M. Martin, Chem. Phys. Lett. **308**, 373 (1999).
[18] V. R. Bhardwaj, F. A. Rajgara, K. Vijayalakshmi, V. Kumarappan, D. Mathur, and A. K. Sinha, Phys. Rev. A **58**, 3849 (1998).
[19] A. Talebpour, S. Larochelle, and S. L. Chin, J. Phys. B **31**, 2769 (1998).
[20] S. Couris, E. Koudoumas, S. Leach, and C. Fotakis, J. Phys. B **32**, L439 (1999).
[21] S. L. Chin and P. A. Golovinski, J. Phys. B **28**, 55 (1995).
[22] Y. Liang, S. Augst, S. L. Chin, Y. Beaudoin, and M. Chaker, J. Phys. B **27**, 5119 (1994).
[23] Y. Liang, A. Talebpour, C. Y. Chien, S. Augst, and S. L. Chin, J. Phys. B **30**, 1369 (1997).
[24] C. Lyngå, A. L'Huillier, and C.-G. Wahlström, J. Phys. B **29**, 3293 (1996).
[25] C.-G. Wahlström, Phys. Scr. **49**, 201 (1994).
[26] A. S. Aleksandrovsky, S. V. Karpov, S. A. Myslivets, A. K. Popov, and V. V. Slabko, J. Phys. B **26**, 2965 (1993).
[27] D. J. Fraser, M. H. R. Hutchinson, J. P. Marangos, Y. L. Shao, J. W. G. Tisch, and M. Castillejo, J. Phys. B **28**, L739 (1995).
[28] X. F. Li, A. L'Huilier, M. Ferray, L. A. Lompre, and G. Mainfray, Phys. Rev. A **39**, 5751 (1989).
[29] Ph. Balcou, C. Cornaggia, A. S. L. Gomes, L. A. Lompre, and A. L'Huilier, J. Phys. B **25**, 4467 (1992).
[30] C.-G. Wahlström, J. Larsson, A. Persson, T. Starczewski, S. Svanberg, P. Salieres, Ph. Balcou, and A. L'Huillier, Phys. Rev. A **48**, 4709 (1993).
[31] D. J. Fraser and M. H. R. Hutchinson, J. Mod. Opt. **43**, 1055 (1996).
[32] N. H. Burnett, C. Kan, and P. B. Corkum, Phys. Rev. A **51**, R3418 (1995).
[33] S. Augst, D. D. Meyerhofer, D. Strickland, and S. L. Chin, J. Opt. Soc. Am. B **8**, 858 (1991).
[34] M. V. Ammosov, N. B. Delone, and V. P. Krainov, Zh. Eksp. Teor, Fiz. **91**, 2008 1986 [Sov. Phys. JETP **64**, 1191 (1986)].
[35] J. W. G. Tisch, T. Ditmire, D. J. Fraser, N. Hay, M. B. Mason, E. Springate, J. P. Marangos, and M. H. R. Hutchinson, J. Phys. B **30**, L709 (1997).
[36] Ph. Balcou and A. L'Huilier, Phys. Rev. A **47**, 1447 (1993).
[37] G. Herzberg, *Electronic Spectra of Polyatomic Molecules* (Van Nostrand, New York, 1966), p. 665.
[38] K. Miyazaki, J. Nonlinear Opt. Phys. Mater. **4**, 567 (1995).
[39] M. Plummer and J. F. McCann, J. Phys. B **28**, L19 (1995).
[40] M. B. Robin, *Higher Excited States of Polyatomic Molecules* (Academic, London, 1985), Vol. III, p. 103.